

Templateless, Surfactantless, Electrochemical Route to a Cuprous Oxide Microcrystal: From Octahedra to Monodisperse Colloid Spheres

Shaojun Guo,^{†‡} Youxing Fang,^{†‡} Shaojun Dong,^{*†} and Erkang Wang[†]

State Key Laboratory of Electroanalytical Chemistry, Changchun Institute of Applied Chemistry, Chinese Academy of Sciences, Changchun 130022, Jilin, China, and Graduate School of the Chinese Academy of Sciences, Beijing 100039, People's Republic of China

Received August 14, 2007

Herein we report a simple electrochemical route for the controlled synthesis of a Cu₂O microcrystal from perfect octahedra to monodisperse colloid spheres via control of the electrodeposition potential without the introduction of any template or surfactant. Perfect Cu₂O octahedra and monodisperse colloid spheres have been obtained in high yield (~100%).

Recently, the synthesis of inorganic nanocrystals of controlled size and shape has gained considerable interest because of their morphology- and size-dependent properties and widespread potential applications in many fields such as catalysis, sensors, nanoelectronics, nanomedicine, and others.¹ To date, many efforts have been devoted to the synthesis of inorganic nanocrystals with different morphologies such as wires,² rods,³ cubes,⁴ hollow spheres, belts,⁵ heterostructures,⁶ etc. However, the preparation of nanocrystals of highly symmetric platonic shapes including tetrahedron, octahedron, hexahedron (cube), icosahedron, and dodecahedron is still a great challenge.

Cuprous oxide (Cu₂O), a p-type semiconductor with a direct band gap of about 2.17 eV, has potential applications in solar energy conversion, electronics, magnetic storage, catalysis, lithium ion batteries, and gas sensors.⁷ In the past decade, several reports have been mentioned with regards to the shape-controlled synthesis of Cu₂O micro- and

nanocrystals such as liquid-phase synthesis of Cu₂O nanowires,⁸ nanocubes,⁹ multipods,¹⁰ pyramids,^{10b} and electrodeposition methods for Cu₂O nanocubes.¹¹ Although Cu₂O crystals with various morphologies have been successfully synthesized, there are few papers that have reported on the preparation of octahedral Cu₂O.^{11,12} Siegfried and Choi^{12a} demonstrated a methodological approach for utilizing the preferential adsorption of surfactant during the electrodeposition process (galvanostatic) to obtain octahedral Cu₂O crystals. However, a great deal of impurities (surfactant) will be introduced onto the surface of a Cu₂O microcrystal. So, it is necessary to develop an effective and facile method (potentiostatic) for the controlled synthesis of a perfect Cu₂O microcrystal with high yield without any surfactant. Herein we report a simple electrochemical route for the controlled synthesis of a Cu₂O microcrystal from perfect octahedra to monodisperse colloid spheres via control of the electrodeposition potential without introduction of any template or surfactant. Perfect Cu₂O octahedra and monodisperse colloid spheres have been obtained in high yield (~100%).

For a typical synthesis of Cu₂O, a 25 mM Cu(OH)₄²⁻ aqueous solution was first prepared using reagent-grade chemicals with distilled water. That is, the solid sodium hydroxide was slowly added to a Cu(NO₃)₂ aqueous solution until the sedimentation [Cu(OH)₂] completely dissolved. Tin-doped indium oxide on glass (ITO; Shenzhen Hivac Vacuum Photoelectronics Co. Ltd.) used as the working electrode was cleaned by sequential sonication in acetone, 10% NaOH in ethanol, and distilled water for 10 min each. The clean Pt wire and Ag/AgCl (saturated KCl) reference electrodes were used as counter and reference electrodes, respectively. The amperometric *i*-*t* curve technique was employed to cause electrochemical deposition of octahedral Cu₂O with a

* To whom correspondence should be addressed. E-mail: dongsj@ciac.jl.cn.

[†] Chinese Academy of Sciences.

[‡] Graduate School of the Chinese Academy of Sciences.

- (1) (a) Jiang, P.; Bertone, J. F.; Colvin, V. L. *Science* **2001**, *291*, 453. (b) Huang, Y.; Duan, X.; Cui, Y.; Lauhon, L.; Kim, K.; Lieber, C. M. *Science* **2001**, *294*, 1313. (c) Puntero, V. F.; Krishnan, K. M.; Alivisatos, A. P. *Science* **2001**, *291*, 2115. (d) Chen, J.; Wang, D.; Xi, J.; Au, L.; Siekkinen, A.; Warsen, A.; Li, Z.-Y.; Zhang, H.; Xia, Y.; Li, X. *Nano Lett.* **2007**, *7*, 1318.
- (2) Tang, Z.; Kotov, N. A.; Giersig, M. *Science* **2002**, *297*, 237.
- (3) Kim, F.; Song, J. H.; Yang, P. *J. Am. Chem. Soc.* **2002**, *124*, 14316.
- (4) Sun, Y.; Xia, Y. *Science* **2002**, *298*, 2176.
- (5) Pan, Z. W.; Dai, Z. R.; Wang, Z. L. *Science* **2001**, *291*, 1947.
- (6) Milliron, D. J.; Hughes, S. M.; Cui, Y.; Manna, L.; Li, J.; Wang, L.; Alivisatos, A. P. *Nature* **2004**, *430*, 190.
- (7) (a) Liu, R.; Kulp, E. A.; Oba, F. E.; Bohannan, W.; Ernst, F.; Switzer, J. A. *Chem. Mater.* **2005**, *17*, 725. (b) Chang, Y.; Teo, J. J.; Zeng, H. C. *Langmuir* **2005**, *21*, 1074. (c) Poizot, P.; Laruelle, S.; Grugeon, S.; Dupont, L.; Taraccon, J. M. *Nature* **2000**, *407*, 496.

- (8) Wang, W. Z.; Wang, G. H.; Wang, X. S.; Zhan, Y. J.; Liu, Y. K.; Zheng, C. L. *Adv. Mater.* **2002**, *14*, 67.
- (9) (a) Gou, L. F.; Murphy, C. J. *Nano Lett.* **2003**, *3*, 231. (b) Liu, R.; Oba, F.; Bohannan, E. W.; Ernst, F.; Switzer, J. A. *Chem. Mater.* **2003**, *15*, 4882. (c) Wang, D.; Mo, M.; Yu, D.; Xu, L.; Li, F.; Qian, Y. *Cryst. Growth Des.* **2003**, *3*, 717.
- (10) Chang, Y.; Zeng, H. C. *Cryst. Growth Des.* **2004**, *4*, 273.
- (11) Li, H.; Liu, R.; Zhao, R.; Zheng, Y.; Chen, W.; Xu, Z. *Cryst. Growth Des.* **2006**, *6*, 2795.
- (12) (a) Siegfried, M. J.; Choi, K. S. *Adv. Mater.* **2004**, *16*, 1743. (b) Siegfried, M. J.; Choi, K. S. *Angew. Chem., Int. Ed.* **2005**, *44*, 3218. (c) Xu, H.; Wang, W.; Zhu, W. *J. Phys. Chem. B* **2006**, *110*, 13829.

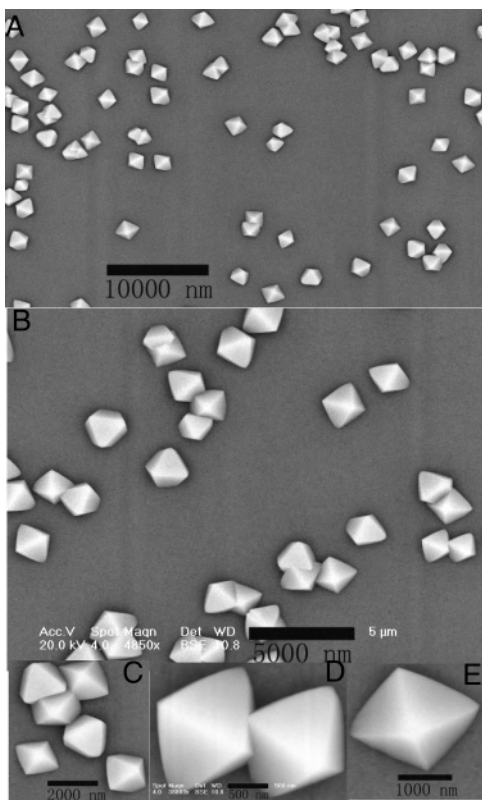


Figure 1. Typical FE-SEM images of octahedral Cu_2O located at the ITO substrate at different magnifications (the deposition time is 15 min; the concentration of $\text{Cu}(\text{OH})_4^{2-}$ is 25 mM).

potential of -0.5 V at room temperature (about 20 °C). A typical chronoamperometric curve is shown in Figure S1 in the Supporting Information.

The morphology of the product was characterized with a XL30 ESEM FEG scanning electron microscopy (SEM) at an accelerating voltage of 15 kV (Figure 1). The lower magnification image (Figure 1A) indicates that the product consists of a large amount of particles, while the higher magnification image (Figure 1B) clearly reveals that the particles are of polyhedral shape. Further magnified images (Figure 1C–E) indicate that these polyhedral particles are perfect octahedra with a size of 1.5 μm and are composed of eight perfect triangle planes.

The chemical composition of octahedral Cu_2O was determined by energy-dispersive X-ray spectroscopy (EDX; Figure S2 in the Supporting Information). The EDX spectrum with two main Cu peaks was observed (other peaks originated from the ITO glass substrate), indicating that the octahedra were made up of Cu. X-ray photoelectron spectroscopy (XPS) was further employed to investigate the composition and valence state of octahedral Cu_2O . Figure S3 in the Supporting Information shows the photoelectron spectrum of $\text{Cu} 1_{2p}$, corresponding to the binding energy of $\text{Cu}^{3/2}_{2p}$ and $\text{Cu}^{1/2}_{2p}$, which is in good agreement with the data observed for Cu_2O .^{8,13} Thus, the XPS result proves that the sample is composed of Cu_2O .

The X-ray diffraction (XRD) analysis of the octahedral Cu_2O was carried out on a D/MAX 2500 V/PC X-ray

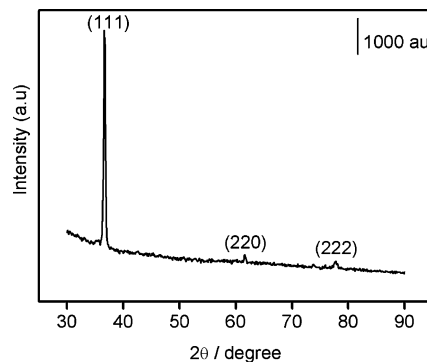


Figure 2. XRD pattern of octahedral Cu_2O located at the ITO substrate.

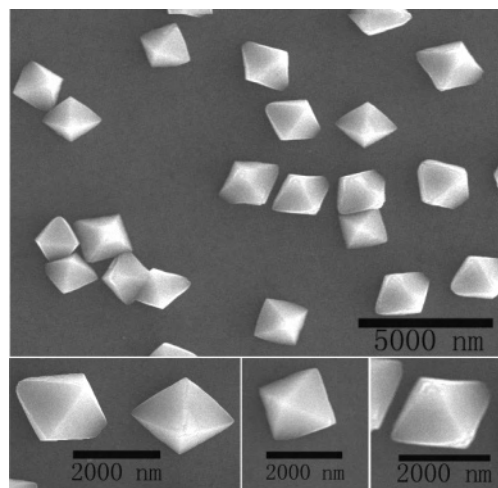


Figure 3. Typical FE-SEM images of octahedral Cu_2O located at the ITO substrate at different magnifications (the deposition time and potential are 15 min and -0.6 V, respectively; the concentration of $\text{Cu}(\text{OH})_4^{2-}$ is 25 mM).

diffractometer using Cu (40 kV and 30 mA) radiation. Figure 2 shows an XRD pattern of the octahedral Cu_2O . The XRD pattern shows sharp peaks corresponding to the (111), (220), and (222) diffraction peaks of Cu_2O . No other diffraction peaks arising from possible impurities such as Cu and $\text{Cu}(\text{OH})_2$ are detected, indicating that the product is composed of pure crystalline Cu_2O . Note that the ratio of the intensity between the (220) and (111) diffraction peaks is much lower than that of the standard file (JCPDS; 0.03 vs 0.27). These observations confirm that octahedral Cu_2O is primarily dominated by (111) facets. Thus, it can be concluded that each triangle facet of octahedral Cu_2O is a (111) facet.

Actually, during the electrodeposition process, the electrodeposition potential affects the morphology and size of the resulting products. When the deposition potential was set at -0.6 V for 15 min, perfect Cu_2O octahedra could still be obtained (Figure 3). However, the size of the octahedra reached to about 2 μm . When the electrodeposition potential was further decreased to -0.7 V, a great deal of monodisperse Cu_2O colloid spheres with diameter of about 500 nm could be obtained (Figure 4). This indicated that the electrochemical preparation of octahedral Cu_2O was probably affected by the kinetic control. In addition, the effect of the concentration of $\text{Cu}(\text{OH})_4^{2-}$ on the resulting morphology was also investigated at the electrodeposition potential of -0.5 V for 15 min. When the concentration of $\text{Cu}(\text{OH})_4^{2-}$ was changed to 50 mM, the octahedra with the bigger size

(13) Lu, C.; Qi, L.; Yang, J.; Wang, X.; Zhang, D.; Xie, J.; Ma, J. *Adv. Mater.* **2005**, *17*, 2562.

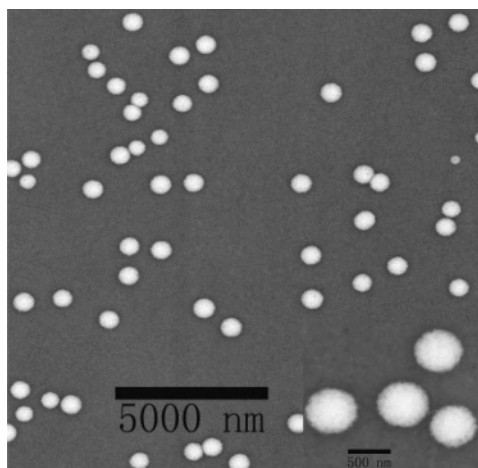
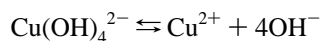


Figure 4. Typical FE-SEM images of octahedral Cu_2O located at the ITO substrate (the deposition time and potential are 15 min and -0.7 V, respectively; the concentration of $\text{Cu}(\text{OH})_4^{2-}$ is 25 mM).

of about $2.5 \mu\text{m}$ could be obtained (Figure S4A in the Supporting Information). Thus, the morphology and size of the Cu_2O particles is tunable via changes in the above parameter.

To further study the growth process of octahedral Cu_2O on the ITO substrate, the morphology of the product obtained from another deposition time (short) was characterized through SEM. Figure S4B in the Supporting Information shows the SEM image of octahedral Cu_2O obtained at -0.5 V for 5 min (the concentration of $\text{Cu}(\text{OH})_4^{2-}$ is 50 mM). It was found that a low density of octahedra with size of about $1 \mu\text{m}$ could be obtained. Thus, the size of Cu_2O octahedra can also be easily controlled via a change in the deposition time.

On the basis of the above observations and references,^{11,12a,c,14} the formation mechanism of the change of morphology of Cu_2O grown on the ITO electrode without any template and surfactant might be explained in terms of the kinetics of the growth process. As is known, the growth rates vary along the different crystallographic directions. The fast growth plane will determine the final morphology.¹⁵ The relative order of the growth rates along the different crystallographic planes can be changed when some organic or inorganic additives are added during the crystal growth process.^{11,12b,c,15} So, selective interactions between additives and a certain facet of nanocrystals will lower the surface energy of the bound plane and hinder the crystal growth perpendicular to this plane, resulting in a change in the final morphology. It is commonly accepted that the shape of the nanocrystal is mainly determined by the ratio (R) of the growth rate along the $[100]$ versus $[111]$ direction.⁴ Tetrahedra and icosahedra bound by the most (111) planes will be formed when R is large (1.73), and perfect cubes bound by the less stable (100) planes will result if R is reduced (0.58). In our electrochemical synthesis system, $\text{Cu}(\text{OH})_4^{2-}$ exists in the following equilibrium:



The Cu^{2+} ion can be slowly reduced to Cu_2O in an alkaline

solution under a certain potential range (from -0.5 to -0.6 V). Also, the OH^- ions might be selectively adsorbed on (111) facets of Cu_2O crystals and slow the growth rates along the $[111]$ direction. This causes the final morphology to appear as octahedra with (111) facets. In addition, several literatures reported that anisotropic nanostructures such as nanoplates, octahedra, tetrahedra, and nanobars could be facilely obtained by operating at a slow reduction rate (the kinetic control).¹⁶ As a comparison, the electrodeposition potential was changed to -0.4 V for 15 min; no particles could be obtained (data not shown). It can be concluded that the reduction potential of $\text{Cu}(\text{OH})_4^{2-}/\text{Cu}_2\text{O}$ is approximately estimated as -0.4 V vs Ag/AgCl (saturated KCl), which is slightly higher than the potential range employed (from -0.5 to -0.6 V). Thus, reduction of $\text{Cu}(\text{OH})_4^{2-}$ will slowly happen in this case. However, changing the electrodeposition potential to -0.7 V will improve the reaction kinetics and result in an increase in the reaction rates. Thus, it is hard to adjust the growth of certain facets of Cu_2O via the OH^- adsorption. Therefore, monodisperse Cu_2O colloid spheres will finally be produced. In addition, the potential-dependent adsorption of OH^- on the preformed Cu_2O facets $[(100)$ and $(111)]$ is probably a key factor. As is known, the change in the concentration of OH^- could be understood via $C(E) = C_0 \exp[nz(E - E_{pzc})/KT]$, where E is the applied potential and E_{pzc} is the potential of zero charge. When the potential was moved to more negative ones, fewer OH^- ions could be adsorbed on the Cu_2O surface because the surface concentration of OH^- is decreased, leading to the formation of spherical particles without preferential growth on certain facets. However, the exact formation mechanism in this synthesis is not quite clear at present and warrants further investigation.

In conclusion, Cu_2O microcrystals from perfect octahedra to monodisperse colloid spheres have been prepared by a simple low-cost electrochemical approach without any template or surfactant. The size of octahedral Cu_2O can be easily controlled via simple control of the deposition time, the electrodeposition potential, and the concentration of $\text{Cu}(\text{OH})_4^{2-}$. Furthermore, the morphology of Cu_2O can be changed to monodisperse colloid spheres when the electrodeposition potential is changed to -0.7 V. In addition, the formation mechanism of Cu_2O microcrystals was primarily discussed. The study is of significance in the shape-controlled synthesis of metal oxide with high yield. More importantly, octahedral Cu_2O microcrystals will probably be useful for a gas sensor, particularly in studying the influence of certain facets $[(111)$ facets] on the performance of the gas sensor.

Acknowledgment. This work was supported by the National Science Foundation of China (Grants 20575064 and 20427003).

Supporting Information Available: Apparatus section and Figures S1–S4. This material is available by free of charge via the Internet at <http://pubs.acs.org>.

IC7016193

(14) Murphy, C. J. *Science* **2002**, *298*, 2139.

(15) Buckley, H. E. *Crystal Growth*; Wiley: New York, 1951.

(16) (a) Xiong, Y.; McLellan, J. M.; Chen, J.; Yin, Y.; Li, Z.-Y.; Xia, Y. *J. Am. Chem. Soc.* **2005**, *127*, 17118. (b) Xiong, Y.; Cai, H.; Wiley, B. J.; Wang, J.; Kim, M. J.; Xia, Y. *J. Am. Chem. Soc.* **2007**, *129*, 3665. (c) Kim, F.; Connor, S.; Song, H.; Kuykendall, T.; Yang, P. *Angew. Chem., Int. Ed.* **2004**, *43*, 3673.